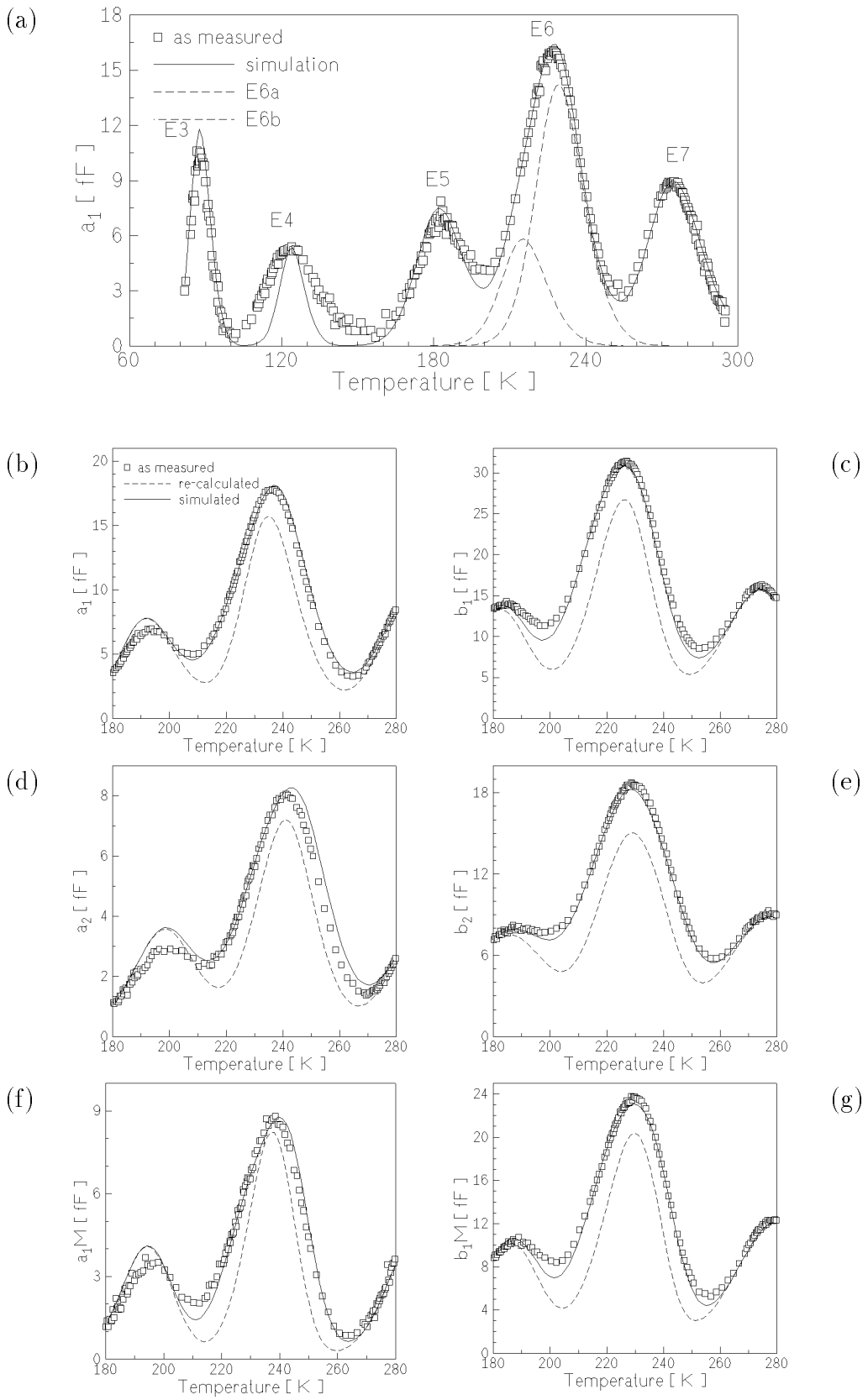

Figure 7.7: (a) : Typical spectrum (t_w = 200 ms) after irradiation (941K11, Φ = $2.88{\cdot}10^{10}$ cm^{-2}). All peaks except E6 were recalculated using the results obtained from this specific measurement. Note that the recalculation of peak E4 with the parameters from the analysis of maxima is not satisfying. Peak E6 is fitted as explained in the text (p. 122). (b-f) : Recalculation and simulation of various coefficients (t_w = 20 ms).

already mentioned in the preceding section. If the sample is cooled under zero bias condition the peak is visible, but if a reverse bias is applied during the cooling no peak occurs in that temperature range (see fig. 7.9).

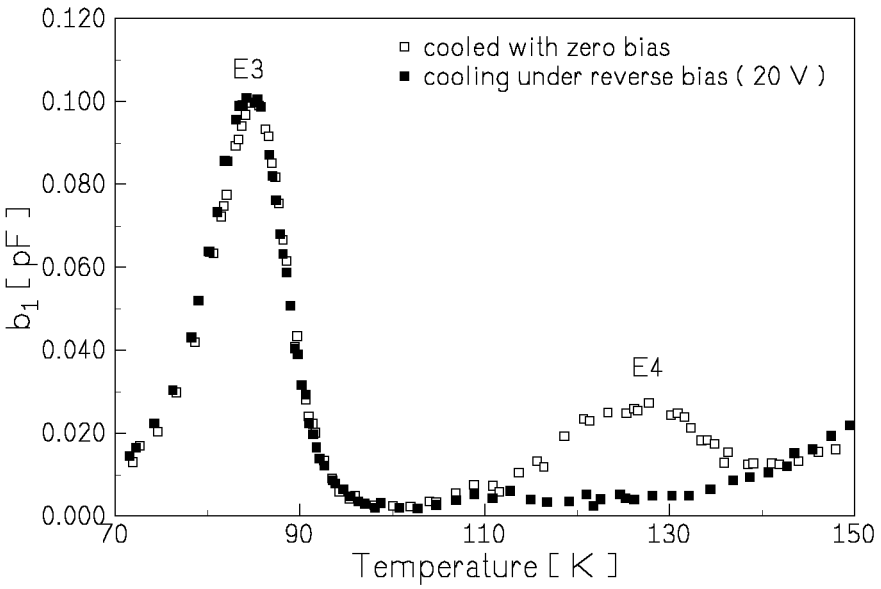

Figure 7.9: Multistable behaviour of peak E4. (911G21, $\Phi = 4.5 \cdot 10^{10}$ cm^{-2})

From all peaks occurring after irradiation only **E3** can be analysed with the direct analysis independent of the material. Since the peak can not be measured completely with the nitrogen cryostat, only the measurements made with the helium cryostat are used to determine the energy level and the cross section of the corresponding energy level. The results as obtained from the direct analysis of measurements performed with various samples are shown in fig. 7.10. It can be seen that the energy level covers a range of about 10 meV. From the linear correlation of $ln(\sigma_n)$ on ΔE_C it follows that the shifts are due to a deviation between the measured temperature and the sample temperature (see sec. 4.2.3, p.51). In addition the level parameters of the same defect as obtained from a TSC-measurement (see fig. 7.19) are also plotted, and found to be in very good agreement with the DLTS-result insofar that $ln(\sigma_n)$ and ΔE_C are correlated rather the same way. Because none of the plotted values can be claimed as correct the centre of the data (excluding the TSC-point) is given here as a result :

$$\Delta E_C = (0.174 \pm 0.003) \text{ eV and } \sigma_n = (1.13 \pm 0.25) \cdot 10^{-14} \text{ cm}^2.$$

It should be emphasised that the errors in ΔE_C and σ_n are not independent, a higher value of ΔE_C corresponds with a higher value of σ_n and vice versa in the case of lower values. The temperature deviation can be calculated, if eqs. 4.39 and 4.41 are resolved to ΔT :

$$\Delta T = T \frac{\Delta E'_T - \Delta E_T}{2\Delta E_T}, \tag{7.1}$$

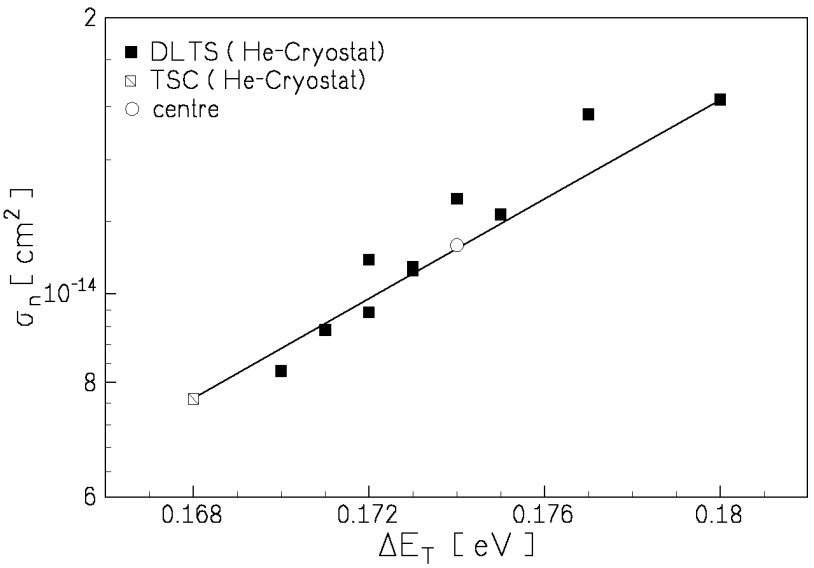

Figure 7.10: Energy level parameters of peak E3 as obtained from various measurements of different samples. From the linear correlation follows that the shifts of the energy level are caused by an error in temperature. The centre has been calculated excluding the value obtained from the TSC-measurement. The straight line covers a temperature range of 3 K.

Label	ΔE_C $[eV]$	σ_n $[cm^2]$	Supposed Identity	Comments	Other Authors [131]	Other Authors [133]	Other Authors [134]
E3	0.174	$1.13{\cdot}10^{-14}$	V-O		0.15 eV	0.18 eV	0.17 eV
E4	0.25	$5{\cdot}10^{-15}$	V-V$^=$	(938 and 933 only)	0.21 eV	0.25 eV	0.25 eV
E6	0.43	10^{-15}	Superposition (see below)		0.39 eV	0.46 eV	
E6a	0.39	$1.2{\cdot}10^{-15}$	V-V$^-$	extracted by fit			0.41 eV
E6b	0.42	$1.0{\cdot}10^{-15}$	(V-P)	extracted by fit			0.46 eV

Table 7.4: Properties of radiation induced peaks. The results of Tokuda and Usamio [131] and Tulach et al. [133] were obtained after neutron exposure, those of Brotherton and Bradley [134] after electron irradiation. The identity of E6b is due to discussion (see sec. 7.1.5). In high resistivity material further levels may contribute to peak E4.

$$\Delta T = T^2 k_B \frac{\ln \sigma' - \ln \sigma}{\Delta E_T}. \tag{7.2}$$

Applying the above given values of ΔE_T and σ_n, and the minimum and maximum values shown in fig. 7.10 the temperature deviation is found to be $\pm$ 1.5 K. T has been assumed to be 85 K.

The determined level parameters are in good agreement with those known from the A-centre (V-O). No evidence has been found whether or not the C_i-C_s-complex, which has the same level parameters (see sec. 3.3), contributes to peak E3.

The number of peaks and the determined energy levels agree with the results obtained by other authors investigating neutron induced energy levels in low resistivity silicon (see tab. 7.4).

7.1.4 Fluence Dependence

For example the DLT-spectra of two different wafers (941 and 938) after various fluences are shown in fig. 7.11. It can be seen clearly that in case of the low resistivity material (938) all peaks increase with fluence. The situation is different for the high resistivity material. For high fluences ($\Phi > 3 \cdot 10^{11}$ cm^{-2}) no peaks below 150 K can be seen. Peak E6 shifts to lower temperature and for $\Phi > 5 \cdot 10^{11}$ cm^{-2} the total spectrum is 'broken down'. This behaviour is a consequence of the temperature and fluence dependence of the effective doping concentration, or the free charge carrier concentration respectively. While N_{eff} decreases with increasing fluence, the trap concentration N_T is assumed to increase in proportion to the fluence. As long as the change in N_{eff} is negligible in comparison to the increase of N_T the peaks will also grow in proportion to the fluence (see fig. 7.11b). But above a certain level of fluence the change of N_{eff} becomes significant. Thus the ratio n_T/N_{eff}[4] which corresponds to the measured quantity (see eq. 4.16) does not grow in proportion to the fluence, but even faster. Although the requirement of $n_T \ll N_{eff}$ is not fulfilled anymore, the measurement of capacitance transients is still possible,[5] and the peaks occurring in the spectra grow also faster (see fig. 7.11a).

The 'break down' of the spectra is correlated with the freezing of charge carriers (see sec. 4.1). Due to the absence of free electrons in the conduction band only the geometrical capacitance can be measured (see sec. 4.1.1), but no transients. The temperature at which the freezing affects the DLTS-measurement depends on N_{eff} and hence also on the fluence. If N_{eff} is sufficient high no freezing occurs in the entire temperature range covered by the DLTS-measurement (see fig. 7.12 case A). With decreasing N_{eff} the 'freezing-temperature' increases and no peaks can be measured in the temperature range below (see fig. 7.12 case B).

The broadening of peak E6 and the shift of the maximum towards lower temperature connected with the 'break-down' of the spectrum in the temperature range below, which has been observed in case of the 941-samples at about $\Phi = 3 \cdot 10^{11}$ cm^{-2} was found also in case of the p$^+$-n -samples. However, the values of fluence and of initial doping concentration $N_{eff,0}$ are a factor of three higher than in case of the high resistivity SB-samples. Thus the ratio of $N_{eff,0}$ to Φ is the same in both cases : $N_{eff,0}/\Phi = 2.3$ cm^{-1}. A similar ratio (2.5 cm^{-1}) can be determined from the 933-material. After $\Phi = 3 \cdot 10^{14}$ cm^{-2} peak E3 could not be analysed and the height of peak E4 was significantly reduced. Hence, it is possible to estimate the maximum neutron fluence Φ_{max}, which can be applied to silicon and which still allows reliable DLTS-measurements by :

$$\Phi_{max} \approx 0.4 \text{ cm} \times N_{eff,0}.$$

[4]Note that n_T is the concentration of occupied traps which is not necessarily equal to N_T.

[5]Note that the application of eqs. 4.24 or 4.25 does not require an exponential behaviour of the transient.

(a)

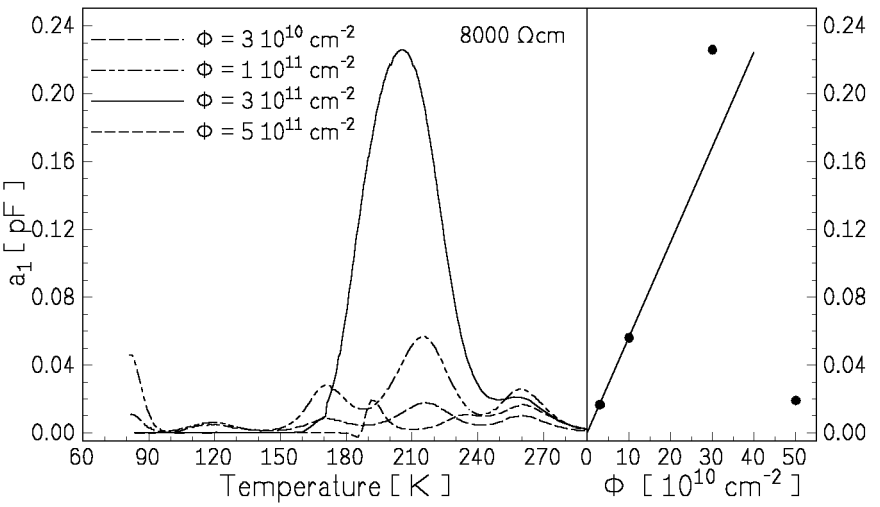

(b)

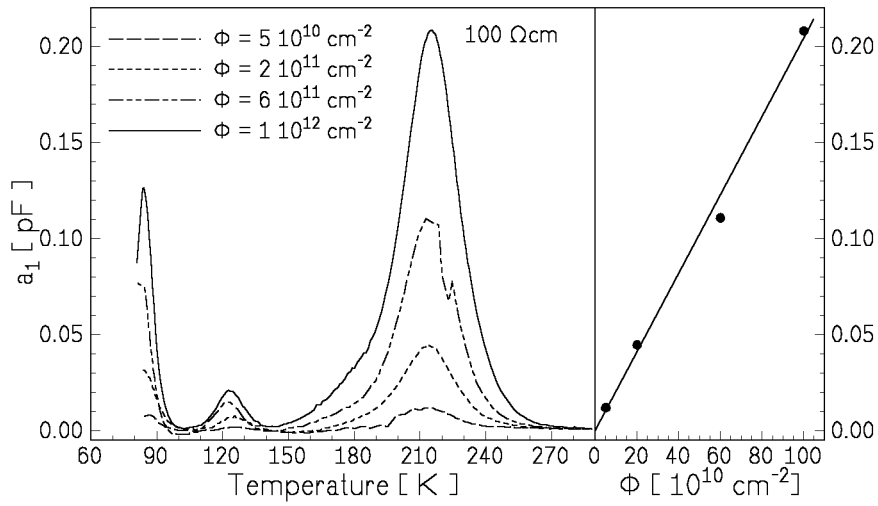

Figure 7.11: Spectra with fluence as parameter. (a) : High resistivity material (941), the seeming increase of the peaks E5 and E7 is caused by the broadening of E6. (b) : low resistivity material (938).

It is hard to give a reasonable explanation for the broadening and the shift because it occurs in the fluence range where the spectra begin to 'break down'. From a straightforward discussion it would be concluded that a further defect level occurs, which contributes on the low temperature side to peak E6. However, a fluence dependence has to be excluded, because the effect does not occur on samples made of low resistivity silicon. Thus the occurrence of such a defect or the possibility of its detection had to depend on the fact that n_T and N_{eff} are of same order of magnitude.

The trap concentrations used for the determination of the generation rates were

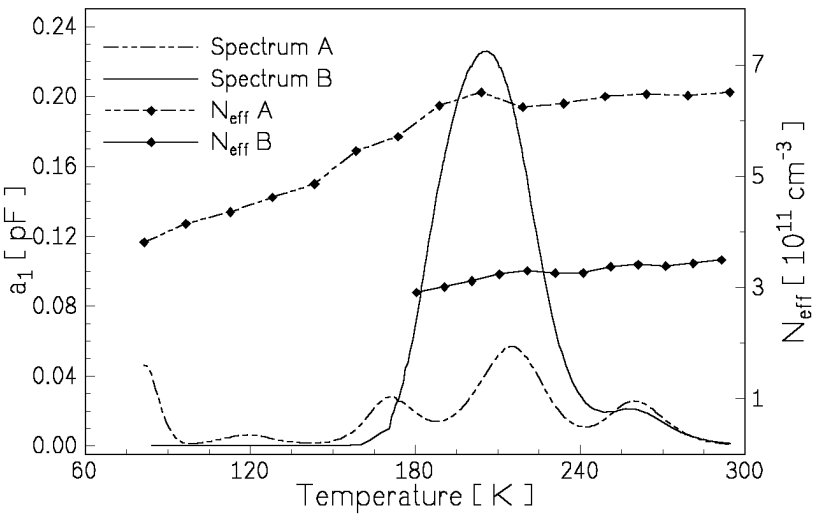

Figure 7.12: Effective doping concentration versus temperature and corresponding spectra. A : Φ = 1.0 $\cdot 10^{11}$ cm^{-2}, and B : Φ = 2.8 $\cdot 10^{11}$ cm^{-2}.

calculated using eq. 4.53. The fraction $\frac{W^2}{W^2+\lambda^2-L_P^2}$ is approximately independent of the doping concentration and thus only the reverse bias voltage V and the filling voltage V_f have to be taken into account. In case of V=20 V and V_f=4 V the fraction is 1.22, and in case of V=10 V and V_f=4 V it is 1.63. In case of V_f=0 V the fraction is approximately 1. Furthermore the temperature dependence of N_{eff} (see sec. 6.1.4) has been taken into account.

In fig. 7.13 for all materials the trap concentration as determined from the corresponding peaks E3, E4, and E6 are shown. In order to separate fluence and annealing effects the room temperature annealing was fixed to about 30 days for all samples. Because only one or two samples per day can be measured, few samples had to be stored at -18°C in order to suppress the annealing processes.

Only measurements of samples exposed to fluences well below the fluence of 'break down' were analysed. It can be seen that the trap concentration depends linearly on the fluence in case of E3 and E6. No significant difference between results obtained from samples of different material can be found, except the p$^+$-n samples. Due to the floating guard-ring the effective area of the electrodes is greater than 0.25 cm^2 and thus by underestimating the volume the determined concentrations are overestimated. Hence, the generation rates were determined as average of all plotted points (n_T/Φ) excluding the values obtained from p$^+$-n samples. The results are listed in tab. 7.5.

The generation rate of the defects corresponding to peak E3 is found to be $g_{E3} = 0.49 \pm 0.12$ cm^{-1} and is in fairly good agreement with the result of Chaudhari et al. [135], who found 0.59 cm^{-1} [6] and assigned the observed peak to the V-O complex.

[6] The value is normalised to 1-MeV equivalent neutron fluence.